Compositional dependence of the soft magnetic properties of the nanocrystalline Fe-Zr-Nb-B alloys with high magnetic flux density

doi: 10.1063/1.372943

Compositional dependence of the soft magnetic properties of the nanocrystalline Fe–Zr–Nb–B alloys with high magnetic flux density

A. Makino and T. Bitoh[a)]
Department of Machine Intelligence and System Engineering, Faculty of System Science and Technology, Akita Prefectural University, Honjo 015-0055, Japan

A. Kojima
Central Research Laboratory, Alps Electric Co., Ltd., Nagaoka 940-8572, Japan

A. Inoue
Institute for Materials Research, Tohoku University, Sendai 980-8577, Japan

T. Masumoto
The Research Institute of Electrical and Magnetic Materials, Sendai 982-0807, Japan

The compositional dependence of the soft magnetic properties of the nanocrystalline Fe–Zr–Nb–B alloys has been investigated. The magnetostriction (λ_s) and the grain size of the $(Fe_{90}Zr_7B_3)_{1-x}(Fe_{84}Nb_7B_9)_x$ alloys, which are two typical ternary alloys mixed with the best soft magnetic properties, show intermediate values between those of the $Fe_{90}Zr_7B_3$ with negative λ_s and the $Fe_{84}Nb_7B_9$ with positive λ_s. However, the soft magnetic properties of the Fe–$(Zr, Nb)_7$–B alloys are inferior to those of the $Fe_{90}Zr_7B_3$ and the $Fe_{84}Nb_7B_9$ alloys. The best soft magnetic properties have been obtained at Zr+Nb=6 at. %. The $Fe_{85.5}Zr_2Nb_4B_{8.5}$ alloy shows a high μ_e of 60 000 at 1 kHz, a high B_s of 1.64 T, and zero λ_s, simultaneously. The alloy also exhibits a very low core loss of 0.09 W/kg at 1.4 T and 50 Hz, which is extremely lower than that of Fe–Si–B amorphous alloys. The nanocrystalline Fe–Zr–Nb–B alloys with improved soft magnetic properties are therefore suitable for pole transformers. © *2000 American Institute of Physics.* [S0021-8979(00)25108-6]

I. INTRODUCTION

Recently, nanocrystalline soft magnetic alloys consisting of α-Fe nanoscale crystallites embedded in a residual amorphous minority matrix have been obtained by crystallizing melt-spun amorphous Fe–M–B (M=Zr, Hf, Nb) ribbons.[1–3] Owing to the strong magnetic coupling between the crystalline grains through the residual ferromagnetic amorphous matrix, the apparent anisotropy is cancelled and the alloys exhibit good soft magnetic properties.[4] The Fe–M–B alloys exhibits a high saturation magnetic flux density (B_s) from 1.5 to 1.7 T as well as good soft magnetic properties.

It is expected that the soft magnetic properties of the Fe–M–B alloys can be improved further by achieving zero magnetostriction (λ_s) because the ternary Fe–M–B alloys show small but nonzero λ_s.[3] In this article, we present the compositional dependence of the soft magnetic properties of the Fe–Zr–Nb–B alloys in the mixed arrangement of the Fe–Zr–B alloy with negative λ_s and the Fe–Nb–B alloy with positive λ_s.

II. EXPERIMENTAL PROCEDURE

Alloy ingots were prepared by arc or induction melting in an Ar atmosphere. A single-roller melt spinning method in an Ar atmosphere was used to produce the rapidly solidified ribbons with 15 mm in width and 20–25 μm in thickness. Annealing treatment of the samples was carried out by treating the samples for 300 s at various temperatures in a vacuum; the heating rate was 3 K/s.

The saturation magnetic flux density (B_s) under an applied field of 800 kA/m and the coercivity (H_c) under a maximum applied field of 800 A/m were measured with a vibrating sample magnetometer (VSM) and a low frequency $B-H$ loop tracer, respectively. The permeability (μ_e) at 1 kHz under an applied field of 0.4 A/m and the core loss (W) at 1.4 T and 50 Hz were measured with a vector impedance analyzer and an ac $B-H$ analyzer operated under sinusoidal input voltage, respectively. The saturation magnetostriction (λ_s) under an applied field of 80 kA/m was measured by a strain gauge technique. The crystallization process of the amorphous alloys was determined by differential thermal analysis (DTA) at a heating rate of 0.17 K/s. The crystallization temperatures (T_x) were determined by onset points of exothermic peaks in DAT curves. The mean grain size (D) was evaluated from the half width of α-Fe (110) x-ray diffraction peak.

III. RESULTS AND DISCUSSION

First, Zr, Nb, and B concentrations were investigated by choosing the $Fe_{90}Zr_7B_3$ and $Fe_{84}Nb_7B_9$ alloys as basic constituents and mixing them in various ratios. In the nanocrystalline Fe–Zr–B and Fe–Nb–B alloys, the compositional range where μ_e shows a maximum does not strictly coincide with the zero λ_s line.[3] The best soft magnetic properties are obtained around the compositions of $Fe_{90}Zr_7B_3$ with negative

a)Electronic mail: teruo_bitoh@akita-pu.ac.jp

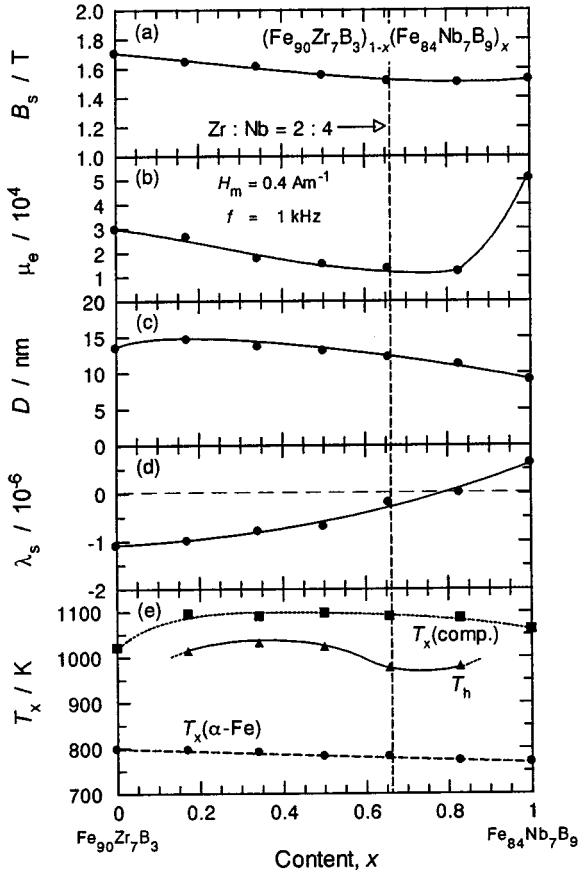

FIG. 1. Compositional dependence of (a) saturation magnetic flux density (B_s), (b) permeability (μ_e), (c) mean grain size (D), (d) magnetostriction (λ_s), and (e) crystallization temperatures (T_x) for nanocrystalline $(Fe_{90}Zr_7B_3)_{1-x}(Fe_{84}Nb_7B_9)_x$ alloys after annealing at the optimum conditions.

λ_s and $Fe_{84}Nb_7B_9$ with positive λ_s. Figure 1 shows the compositional dependence of (a) B_s, (b) μ_e, (c) D, (d) λ_s, and (e) T_x of the $(Fe_{90}Zr_7B_3)_{1-x}(Fe_{84}Nb_7B_9)_x$ alloys as a function of x. The $T_x(\alpha$-Fe) and T_x(comp.) are the temperature where the alloys change the structure from amorphous to α-Fe+amorphous phases, and to α-Fe+compound phases, respectively. The T_h will be discussed hereafter. The saturation magnetic flux density, D, λ_s, and $T_x(\alpha$-Fe) of the $(Fe_{90}Zr_7B_3)_{1-x}(Fe_{84}Nb_7B_9)_x$ alloys show intermediate values between those of the $Fe_{90}Zr_7B_3$ and the $Fe_{84}Nb_7B_9$ alloys. However, μ_e of the $(Fe_{90}Zr_7B_3)_{1-x}(Fe_{84}Nb_7B_9)_x$ alloys are inferior to those of the $Fe_{90}Zr_7B_3$ and the $Fe_{84}Nb_7B_9$ alloys. It is noted that μ_e shows the minimum around $x=0.8$ where the alloy exhibits zero λ_s.

Next, we have studied the effect of Zr+Nb amount on the soft magnetic properties. The best soft magnetic properties have been obtained at Zr+Nb=6 at.%. Figure 2 shows the pseudoternary diagram of μ_e (solid lines), B_s (broken lines), and λ_s (dotted lines) for Fe–(Zr, Nb)–B alloys crystallized under optimum conditions, where the Zr+Nb amount was constant at 6 at.%. The small grain size from 10 to 11 nm have been obtained in a compositional range from 0 to 3 at.% Zr and from 6 to 9 at.% B. The permeability reaches the maximum value of 60 000 for the $Fe_{85.5}Zr_2Nb_4B_{8.5}$ alloy, which shows zero λ_s. It should be

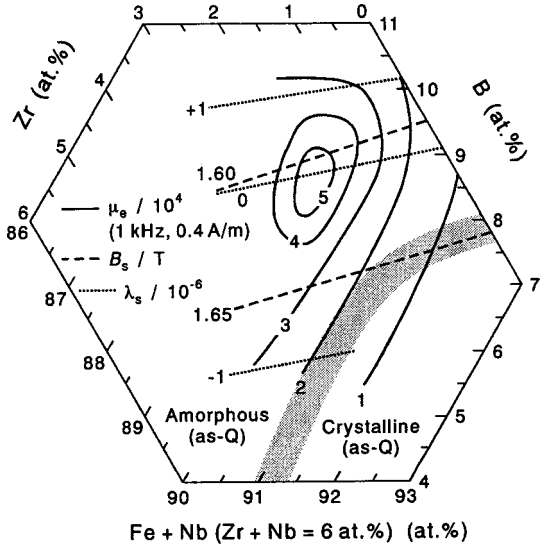

FIG. 2. Pseudoternary diagram of permeability (μ_e), saturation magnetic flux density (B_s) and magnetostriction (λ_s) for nanocrystalline Fe–$(Zr, Nb)_6B$ alloys after annealing at the optimum conditions. The data of the phase field in an as-quenched state are also shown.

noted that the best soft magnetic properties have been obtained around Zr:Nb=2:4 when Zr+Nb=6 at.%. As shown in Fig. 1, μ_e shows the minimum around Zr:Nb=2:4 when Zr+Nb=7 at.%, whereas zero λ_s has been obtained. Figure 3 shows the pseudoternary diagram of W (solid lines) and H_c (broken lines) for Fe–$(Zr, Nb)_6$–B alloys crystallized under optimum conditions. The gray region indicates where the high μ_e values more than 50 000 have been obtained. The extremely low W less than 0.09 W/kg, which is 1/2–2/3 that of the Fe–M–B ternary alloys and is extremely lower than that of amorphous Fe–Si–B alloys, have been obtained in a compositional range of 1.5–2.2 at.% Zr and 8–9 at.% B.

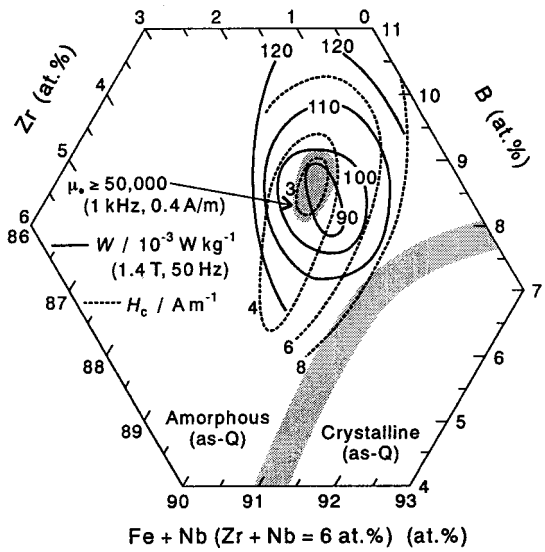

FIG. 3. Pseudoternary diagram of core loss (W) and coercivity (H_c) for nanocrystalline Fe–$(Zr, Nb)_6B$ alloys after annealing at the optimum conditions. The gray area indicates the compositional range obtaining high permeability more than 50 000. The data of the phase field in an as-quenched state are also shown.

TABLE I. Mean grain size (D), saturation magnetic flux density (B_s), permeability (μ_e), coercivity (H_c), magnetostriction (λ_s), and core loss (W) of nanocrystalline Fe–M–B alloys and Fe–Si–B amorphous alloy.

	D (nm)	B_s (T)	μ_e[a]	H_c (A/m)	λ_s (10^{-6})	W[b] (W/kg)
$Fe_{90}Zr_7B_3$	13	1.70	30 000	5.8	−1.1	0.21
$Fe_{84}Nb_7B_9$	9	1.52	51 000	4.8	0.6	0.14
$Fe_{85.5}Zr_2Nb_4B_{8.5}$	11	1.64	60 000	3.0	−0.1	0.09
$(Fe_{90}Zr_7B_3)_{0.17}(Fe_{84}Nb_7B_9)_{0.83}$	11	1.59	12 000	10.0	0	···
$Fe_{78}B_{13}Si_9$ (amor.)	···	1.56	10 000	3.5	27	0.28

[a]1 kHz, 0.4 A/m.
[b]50 Hz, 1.4 T.

The compositional range where W exhibits the minimum extends to lower B content from the region where the best μ_e and H_c values have been obtained. This is due to the increase of B_s with decreasing B content. Since W increases rapidly near magnetic saturation, the higher B_s is favorable to obtaining low W.

The magnetic properties of the nanocrystalline Fe–M–B alloys are summarized in Table I. The $Fe_{85.5}Zr_2Nb_4B_{8.5}$ and $(Fe_{90}Zr_7B_3)_{0.17}(Fe_{84}Nb_7B_9)_{0.83}$ alloys have the same D value of 11 nm and zero λ_s after the crystallization. However, the soft magnetic properties are very different; μ_e of the former alloy is five times as large as that of the latter alloy. Figure 4 shows the DTA curves of the amorphous $Fe_{85.5}Zr_2Nb_4B_{8.5}$ and $(Fe_{90}Zr_7B_3)_{0.17}(Fe_{84}Nb_7B_9)_{0.83}$ alloys. The two clear exothermic peaks around 800 and 1100 K, which correspond to the structural changes from amorphous to α-Fe+amorphous phases, and to α-Fe+compound phases, respectively. It should be noted that the small hump around 1000 K, indicated by the arrow, is observed in the DTA curve for the $(Fe_{90}Zr_7B_3)_{0.17}(Fe_{84}Nb_7B_9)_{0.83}$ alloy. Similar humps are observed in the DTA curves for the other Fe–$(Zr, Nb)_7$–B alloys as shown in Fig. 1 (indicated by T_h) and Fe–$(Zr, Nb)_6$–B alloys containing more than 10 at. % B or 3 at. % Zr. It should be noted that the soft magnetic properties of these alloys are inferior. It seems to us that the hump originates from structural or chemical change of the residual amorphous phase. These results imply that the high thermal stability of the residual amorphous phase is necessary to obtain the good soft magnetic properties.

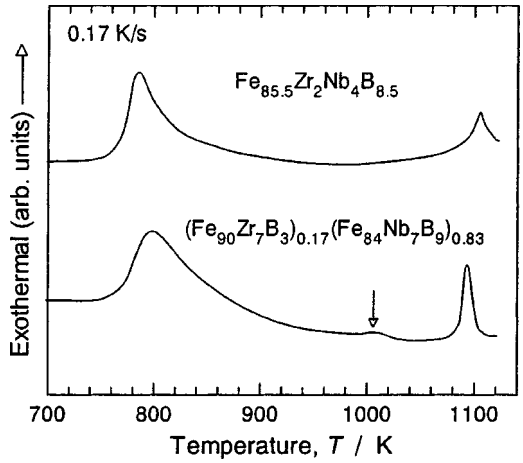

FIG. 4. DTA curves for amorphous $Fe_{85.5}Zr_2Nb_4B_{8.5}$ and $(Fe_{90}Zr_7B_3)_{0.17}(Fe_{84}Nb_7B_9)_{0.83}$ alloys.

As shown in Table I, it is to be noted that the soft magnetic properties of the $Fe_{85.5}Zr_2Nb_4B_{8.5}$ alloy are superior to those of the amorphous $Fe_{78}Si_9B_{13}$ alloy. Furthermore, it has been confirmed that the $Fe_{85.5}Zr_2Nb_4B_{8.5}$ alloy also has a good thermal stability of the magnetic properties.[5] It can be concluded that the nanocrystalline $Fe_{85.5}Zr_2Nb_4B_{8.5}$ alloy with high B_s is suitable for a core material for pole transformers.

IV. CONCLUSION AND FUTURE WORK

The present work reveals the soft magnetic properties of the Fe–Zr–Nb–B alloys are strongly affected by the Zr+Nb amount and the Zr/Nb ratio. This result implies that the chemical interaction between Zr and Nb atoms is important. Further investigations such as a detailed analysis of the crystallization process of the alloys are required to clarify the effect of the mixing of Zr and Nb on the microstructure and the magnetic properties.

ACKNOWLEDGMENT

This work is financially supported by the New Energy and Industrial Technology Development Organization (NEDO).

[1] A. Makino, K. Suzuki, A. Inoue, Y. Hirotsu, and T. Masumoto, J. Magn. Magn. Mater. **133**, 329 (1994).
[2] A. Makino, A. Inoue, and T. Masumoto, Nanostruct. Mater. **6**, 985 (1995).
[3] A. Makino, A. Inoue, and T. Masumoto, Mater. Trans., JIM **36**, 924 (1995).
[4] G. Herzer, IEEE Trans. Magn. **25**, 3327 (1989).
[5] A. Makino, T. Bitoh, A. Kojima, A. Inoue, and T. Masumoto, Proceedings of the 10th International Conference On Rapidly Quenched and Metastable Materials (to be published).